

# Mechanical properties and superstructure of high-modulus and high-strength nylon-6 fibre prepared by the zone-annealing method

Toshio Kunugi, Isamu Akiyama and Minoru Hashimoto

Department of Applied Chemistry, Faculty of Engineering, Yamanashi University, Takeda-4, Kofu, 400 Japan

(Received 10 July 1981)

The relationships between mechanical properties and superstructure of nylon-6 fibre prepared by a new annealing method, called the zone-annealing method, were investigated in comparison with three other annealing methods, namely, annealing under release, annealing at constant length, and annealing under tension. It was found that the very high modulus and strength of the zone-annealed fibre were directly attributed to the large number of tie molecules connecting the crystallites and to the high orientation of the amorphous chains.

**Keywords** High-modulus; high-strength; nylon-6 fibre; zone-annealing; mechanical properties; superstructure

## INTRODUCTION

Recently, we succeeded in preparing high-modulus and high-strength fibre from crystalline polymer, already widely used, by a new annealing method invented by T. Kunugi and coworkers, the 'zone-annealing method'. This method has so far been applied to poly(ethylene terephthalate)<sup>1-6</sup>, nylon-6<sup>5-8</sup>, polyethylene<sup>5,9,10</sup>, and polypropylene<sup>11</sup> in the forms of fibre and film. In spite of the very simple apparatus and easy procedure employed, the resulting fibre exhibited excellent mechanical properties and high dimensional stability at elevated temperatures.

In the preceding report<sup>7</sup> we briefly interpreted this new method and discussed the application to nylon-6 fibre. It was stated that the dynamic storage modulus of the zone-annealed fibre reached  $10.8 \times 10^{10}$  dyne cm<sup>-2</sup>, 2.2-4.0 times that of the high-tenacity nylon-6 fibre available commercially.

In this report, we deal with the results of subsequent detailed research on the zone-annealed fibre. In particular, the relationship between mechanical properties and superstructure of the zone-annealed fibre are discussed, in comparison with those of fibres prepared by three other annealing methods varying tension and heating area on annealing.

## EXPERIMENTAL

### Material

The original material used in the present study is as-spun nylon-6 fibre of 0.49 mm diameter, supplied by Toray Research Center, Inc. The fibre has a birefringence of  $5 \times 10^{-4}$  and a crystallinity of 27.7%.

### Zone-drawing and zone-annealing

The zone-annealing procedure consists of two stages; zone-drawing and zone-annealing. The zone-drawing was done on the original as-spun fibre in order to produce a

fibre with as high an orientation and as low a crystallinity as possible, whereas the zone-annealing was subsequently carried out to convert the zone-drawn fibre into a fibre with a high orientation and a high crystallinity.

The apparatus used here is the usual tensile tester partially reconstructed. A band heater 2 mm wide was attached to the movable crosshead. The temperature of the band heater can be held constant throughout the experimental period by a control system. The upper end of the fibre was fixed and the desired tension was applied to the lower end by weighting. The band heater can be moved up or down along the fibre axis at a moving speed chosen from 2, 4, 8, 10, 20, or 40 mm min<sup>-1</sup>.

In this study, the zone-drawing and zone-annealing were performed under the conditions determined in the previous report<sup>7</sup>. The conditions are shown in *Table 1*.

### Other annealing methods

To elucidate the characteristic effectiveness of the zone-annealing method, the mechanical properties and superstructure of the zone-annealed fibre were compared with those of the fibres prepared by three other annealing methods: annealing under release, annealing at constant

*Table 1* The most suitable conditions for zone-drawing and zone-annealing

Conditions	Zone-drawing	Zone-annealing
Temperature of the heating zone (°C)	80	180
Moving speed of the band heater (mm min <sup>-1</sup> )	40	10
Moving direction of the band heater	up	up or down
Tension applied to the fibre (kg mm <sup>-2</sup> )	1.6	15.8
Repetition (times)	1	6

**Table 2** Mechanical properties of the fibres prepared by the four kinds of annealing methods

Sample	Young's modulus ( $\times 10^{-10}$ dyne $\text{cm}^{-2}$ )	Strength at break ( $\text{kg mm}^{-2}$ )	Elongation at break (%)
Fibre annealed under release	3.71	50.0	53.8
Fibre annealed at constant length	4.12	55.2	38.1
Fibre annealed under tension	5.73	62.6	12.5
Fibre zone-annealed	9.91	100.3	13.6

length, and annealing under tension. The annealing under release and the annealing at constant length were carried out at 180°C for 30 min in 3 mmHg vacuum on the fibres previously cold-drawn up to 3-fold at room temperature. The annealing under tension was carried out at 175°C for 30 min in an air oven under a tension of 9  $\text{kg mm}^{-2}$  on the fibre cold-drawn up to 3-fold. This draw ratio, 3-fold, is almost identical with the draw ratio obtained by zone-drawing, 2.9-fold. However, the tension, 9  $\text{kg mm}^{-2}$ , differs widely from the tension used at zone-annealing, 15.8  $\text{kg mm}^{-2}$ .

Although, in the case of PET fibre<sup>2</sup>, both annealings were done under the same tension and at the same temperature, in the case of nylon-6 fibre, the tension of 15–16  $\text{kg mm}^{-2}$  could not be applied to the fibre in the air oven for 30 min because of severance. The zone-annealing under the tension of 9  $\text{kg mm}^{-2}$  was also carried out. The data of the obtained fibre, however, were omitted, because the mechanical properties were only slightly inferior to, but similar to those of the fibre zone-annealed under 15.8  $\text{kg mm}^{-2}$ .

#### Measurements

The mechanical properties of the fibres thus prepared were measured with a tensile strength tester and a viscoelastometer. The tensile properties were determined at 23–25°C, RH 65%, on a monofilament 20 mm long. Young's modulus, tensile strength, and elongation at break were estimated from the stress-strain curves. The dynamic viscoelastic properties,  $E'$ ,  $E''$ , and  $\tan \delta$  were measured at 110 Hz on 20 mm long fibres. The measurement was carried out in two temperature ranges: one from room temperature to -140°C and the other from room temperature to 180°C. In the former range the experiments were performed at a cooling rate of 2°C  $\text{min}^{-1}$  in a stream of dry air cooled with liquid nitrogen, and in the latter range at a heating rate of 1.5°C  $\text{min}^{-1}$  in a stream of dry nitrogen gas.

The density of the fibres ( $d$ ) was measured at 25°C by a flotation method using toluene-carbon tetrachloride mixtures. From the obtained density, the degree of crystallinity ( $X_c$ ) was calculated by the usual method using a crystal density<sup>12</sup> of 1.230 and an amorphous region density<sup>13</sup> of 1.084  $\text{g cm}^{-3}$ .

The birefringence ( $\Delta_t$ ) was measured with a polarizing microscope equipped with the Berek compensator. In the measurements on the fibres with high retardation, X-Z planes of various thicknesses which were cut from a single crystal of quartz were simultaneously used as additional compensators. The orientation factor of the crystallites

( $f_c$ ) was determined by an X-ray diffraction method proposed in a previous paper<sup>14</sup>. Further, the orientation factor of the amorphous chains ( $f_a$ ) was calculated from the following equation by substituting the values of  $X_c$ ,  $\Delta_t$ , and  $f_c$  measured separately.

$$f_a = \frac{\Delta_t - \Delta_c^{\circ} f_c X_c}{\Delta_a^{\circ} (1 - X_c)}$$

where  $\Delta_c^{\circ}$  and  $\Delta_a^{\circ}$  are the intrinsic birefringences of the crystal<sup>15</sup> and amorphous phase<sup>15</sup>, 0.0780 and 0.0689, respectively.

## RESULTS AND DISCUSSION

### Mechanical properties

The tensile properties of the fibres prepared by the four kinds of annealing methods are compared in Table 2. Young's modulus of the zone-annealed fibre is significantly higher than those of the fibres annealed in the other ways and corresponds to about 6% of the crystal modulus<sup>16</sup> along the molecular chains, 165  $\times 10^{10}$  dyne  $\text{cm}^{-2}$ . From the Table, it can also be seen that Young's modulus, and strength at break, increase in the order of the fibre annealed under release, one annealed at constant length, one annealed under tension, and one zone-annealed. This indicates that these mechanical properties can be improved by increasing the tension during annealing and that in spite of short heating-time the annealing at a narrow zone of the fibre is far more effective than that over the whole fibre.

Figures 1 and 2 show the temperature dependences of the dynamic storage modulus,  $E'$ , in the two temperature ranges. It should be emphasized that the  $E'$  value of the zone-annealed fibre is again highest over the whole temperature range and maintains a high level at elevated temperatures. For example, it shows an  $E'$  value of 5.5  $\times 10^{10}$  dyne  $\text{cm}^{-2}$  even at 180°C. In addition, the  $E'$  value at room temperature, 10.8  $\times 10^{10}$  dyne  $\text{cm}^{-2}$ , is 2.2–4.0 times that of the high-tenacity fibre available commercially, 2.7–5.0  $\times 10^{10}$  dyne  $\text{cm}^{-2}$ , as described in the preceding paper<sup>7</sup>.

### Orientation and crystallinity

Table 3 shows the birefringence ( $\Delta_t$ ), orientation factors of crystallites and amorphous chains ( $f_c$  and  $f_a$ ), and

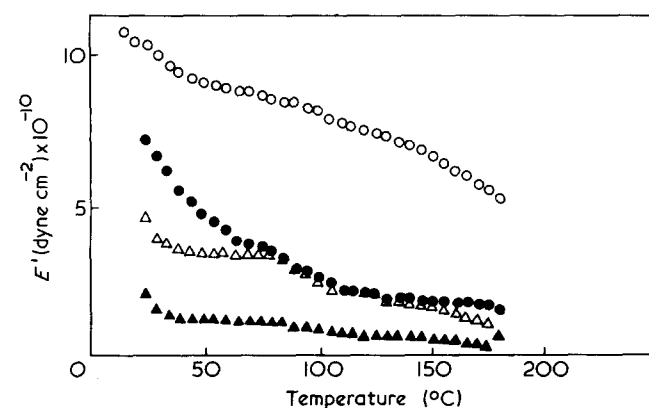


**Figure 1** Temperature dependence of dynamic storage modulus  $E'$  in the higher temperature range for the fibre annealed under release ( $\Delta$ ), fibre annealed at constant length ( $\triangle$ ), fibre annealed under tension ( $\bullet$ ), and fibre zone-annealed ( $\circ$ )

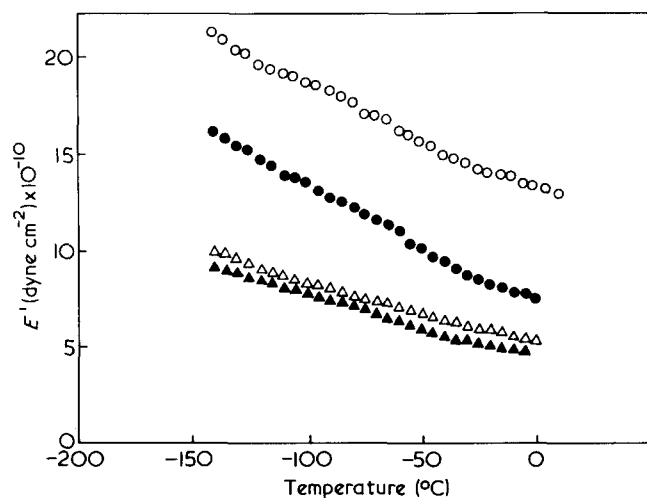


Figure 2 Temperature dependence of dynamic storage modulus  $E'$  in the lower temperature range for the fibre annealed under release (▲), fibre annealed at constant length (△), fibre annealed under tension (●), and fibre zone-annealed (○)

Table 3 Birefringence ( $\Delta_t$ ), orientation factors of crystallites and amorphous chains ( $f_c$  and  $f_a$ ), and crystallinity ( $X_c$ ) for the fibres prepared by the four kinds of annealing methods

Sample	$\Delta_t$ ( $\times 10^3$ )	$f_c$	$f_a$	$X_c$
Fibre annealed under release	50.7	0.878	0.506	47.0
Fibre annealed at constant length	53.1	0.905	0.550	46.4
Fibre annealed under tension	58.7	0.885	0.714	47.7
Fibre zone-annealed	60.3	0.849	0.792	48.9

crystallinity ( $X_c$ ) for the four kinds of fibres. The values of  $\Delta_t$  and  $f_a$  are arranged in the same order as in the case of the mechanical properties. This suggests that the orientation, especially the orientation of amorphous chains, plays an important role in the improvement of the mechanical properties. However, the magnitude of  $f_c$  and  $X_c$  cannot be directly related to the mechanical properties, because these values are irregularly aligned. Particularly, Young's modulus and the tensile strength of the fibre annealed under release are only 37% and 50% of those of the zone-annealed fibre, respectively, in spite of the high values of  $f_c$  and  $X_c$  comparable with those of the zone-annealed fibre. This indicates that the crystalline portion of the fibre annealed under release consists of lamellae which are not very useful in transmitting the force. Thus, the structure rather than the quantity of crystallites is far more important for the improvement of the mechanical properties.

#### Mechanical dispersion peaks

The temperature dependences of  $\tan \delta$  and  $E''$  in the two temperature ranges are shown in Figures 3, 4, 5 and 6. Three distinct dispersion peaks appear at 75°–95°C, ~ -50°C and ~ -130°C. As is well known, these peaks are  $\alpha$ ,  $\beta$  and  $\gamma$  dispersion peaks, respectively. Only the dispersion curve of the fibre annealed under tension is irregular in the higher temperature range (Figures 3 and 5). The abnormal behaviour appears to be due to the weak air-oxidation of the fibre during annealing. In other fibres, however, the  $\alpha$  dispersion peak becomes progressively

smaller and broader and shifts to higher temperatures in the order described above. The temperature positions of the  $\alpha$  dispersion peaks are also listed in Table 4. From the comparison of the intensity and temperature of the peak, it is found that the movement of the amorphous molecular chains at the  $\alpha$  dispersion temperature range becomes progressively more difficult in the same order.

The temperature positions of the  $\beta$  and  $\gamma$  dispersion peaks, however, are virtually unaffected by the differences in the annealing methods as seen in Figures 4 and 6. We reported<sup>17</sup> that the temperature positions of the  $\beta$  and  $\gamma$  dispersion peaks were not very sensitive to the variation in the superstructure of nylon-6 fibre, on the basis of the viscoelastic data for 15 kinds of nylon-6 fibres which were prepared by various combinations of cold-drawing and annealing.

However, the intensities of the  $E''$  peaks of all dispersions increase regularly in the same order (Figures 5

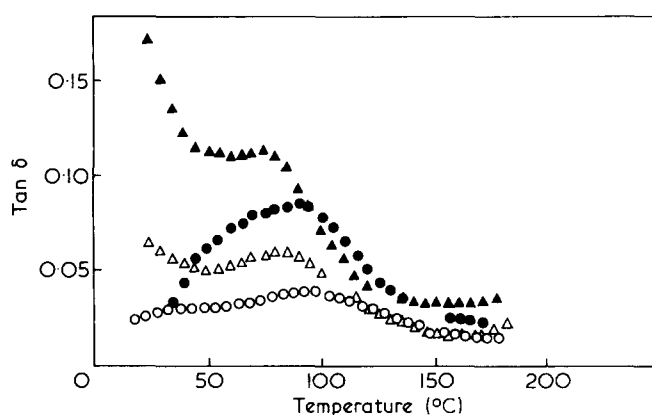


Figure 3 Temperature dependence of  $\tan \delta$  in the higher temperature range for the fibre annealed under release (▲), fibre annealed at constant length (△), fibre annealed under tension (●), and fibre zone-annealed (○)

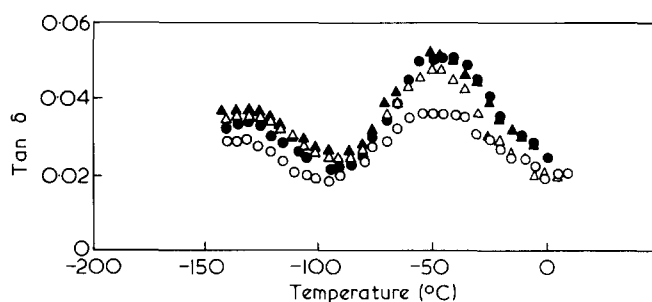


Figure 4 Temperature dependence of  $\tan \delta$  in the lower temperature range for the fibre annealed under release (▲), fibre annealed at constant length (△), fibre annealed under tension (●), and fibre zone-annealed (○)

Table 4 Peak temperatures of  $\alpha$  dispersion for the fibres prepared by the four kinds of annealing methods

Sample	Peak temperatures of $\alpha$ dispersion (°C)	
	$E''$	$\tan \delta$
Fibre annealed under release	75	75
Fibre annealed at constant length	78	83
Fibre annealed under tension	(50)	88
Fibre zone-annealed	96	95

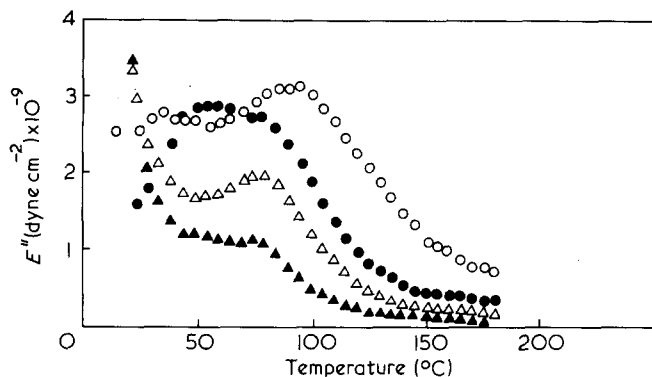


Figure 5 Temperature dependence of loss modulus  $E''$  in the higher temperature range for the fibre annealed under release ( $\blacktriangle$ ), fibre annealed at constant length ( $\triangle$ ), fibre annealed under tension ( $\bullet$ ), and fibre zone-annealed ( $\circ$ )

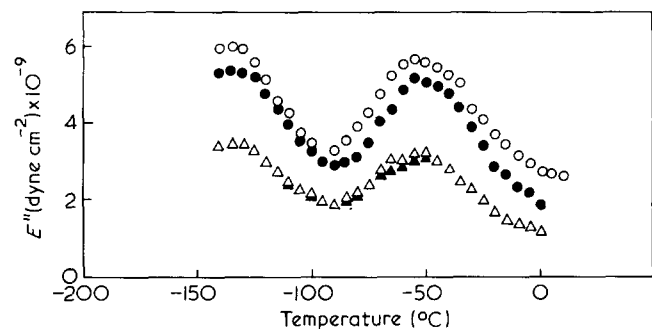


Figure 6 Temperature dependence of loss modulus  $E''$  in the lower temperature range for the fibre annealed under release ( $\blacktriangle$ ), fibre annealed at constant length ( $\triangle$ ), fibre annealed under tension ( $\bullet$ ), and fibre zone-annealed ( $\circ$ )

and  $\delta$ ). Since the intensity of the  $E''$  dispersion peak indicates the energy dissipated as frictional heat per cycle in a sinusoidal deformation, the increases in the peak intensities imply increases in intermolecular friction.

On the basis of these experimental results, we assumed that the amorphous region of the zone-annealed fibre consisted of highly oriented and densely aggregated extended molecular bundles. The assumption is also supported by the small-angle X-ray scattering feature of the zone-annealed fibre<sup>7</sup>.

#### Estimation of amorphous modulus and number and fraction of the tie molecules

Unless the crystalline region is completely continuous along the fibre axis, the amorphous region having a lower modulus has a more pronounced influence on the mechanical properties of the whole fibre than that of the crystalline region. Particularly, the orientation of amorphous chains, the number and fraction of tie molecules, and the distribution of length and strain of tie molecules may be considered as important factors concerning the amorphous region. If a uniaxially oriented fibre can be represented by a mechanical structural model in which the crystalline and amorphous regions are alternately arranged in the fibre axis direction, the following equation can be set up for additivity of compliances.

$$\frac{1}{E_{\parallel}} = \frac{X_c}{E_{c\parallel}} + \frac{1-X_c}{E_a}$$

Table 5 Amorphous modulus ( $E_a$ ), number and fraction of the tie molecules ( $(1-X_c)E_{\parallel}/E_{c\parallel}$  and  $\beta E$ ) of the fibres prepared by the four kinds of annealing methods

Sample	$E_a$ ( $\times 10^{-10}$ dyne $\text{cm}^{-2}$ )	$(1-X_c) \frac{E_{\parallel}}{E_{c\parallel}}$	$\beta E$
Fibre annealed under release	1.96	0.012	0.022
Fibre annealed at constant length	2.20	0.013	0.025
Fibre annealed under tension	2.98	0.018	0.035
Fibre zone-annealed	5.22	0.031	0.060

where  $E_{\parallel}$  is the as-measured macromodulus,  $E_{c\parallel}$  is the crystal modulus along the molecular chains, and  $X_c$  is the volume crystallinity. When  $E_{c\parallel} = 165 \times 10^{10}$  dyne  $\text{cm}^{-2}$  and the measured  $X_c$  and  $E_{\parallel}$  are substituted in the above equation, the amorphous modulus ( $E_a$ ) is given for the fibre under consideration. This evaluation of  $E_a$  is based on the idea that even when some fibres have the same value of crystallinity, each fibre may possess a different  $E_a$  value, its magnitude depending on individual superstructure. The values of  $E_a$  are listed in Table 5. The value of  $E_a$  also increases in the same order as in the case of Young's modulus, the strength at break, and the dynamic storage modulus. The discrepancies in the mechanical properties among the four fibres arise mainly from those of the amorphous region.

Subsequently, the number and fraction of tie molecules were estimated by Peterlin's procedure<sup>18</sup>. Under the assumption that the elastic modulus is exclusively caused by tie molecules and that the tie molecules are uniformly distributed and all of equal length, Peterlin<sup>18</sup> stated that the number and fraction of tie molecules could be represented by  $(1-X_c)E_{\parallel}/E_{c\parallel}$  and  $\beta E = E_{\parallel}/E_{c\parallel}$ , respectively. The values obtained for  $(1-X_c)E_{\parallel}/E_{c\parallel}$  and  $\beta E$  are listed in Table 5. These values are again arranged in the same order of increasing magnitude as obtained for Young's modulus, strength at break, dynamic storage modulus, birefringence,  $f_a$  and  $E_a$ . These values are only a measure of the number of tie molecules, because the tie molecules in an actual fibre are of unequal length and are nonuniformly strained upon loading. However, it is certain that the zone-annealed fibre contains a large number of tie molecules. The large number of tie molecules contributes to the increase in  $E_a$ , and then the increase in  $E_a$  results in an increase in the macroscopic modulus and the strength of the whole fibre. This conclusion is identical with that obtained for poly(ethylene terephthalate) fibre in a preceding study<sup>2</sup>.

#### CONCLUSION

The zone-annealing procedure is effective for the formation of an extended-chain structure, and consequently the obtained fibre exhibits excellent mechanical properties.

#### ACKNOWLEDGEMENTS

The authors wish to thank Prof. Kei Matsuzaki, University of Tokyo, for his valuable comments and helpful suggestions. Thanks are also due to the financial support by the grant from the scientific research funds (Kagaku Kenkyu-hi) of the Ministry of Education, Japan.

REFERENCES

- 1 Kunugi, T., Suzuki, A. and Hashimoto, M. *J. Appl. Polym. Sci.* 1981, **26**, 213
- 2 Kunugi, T., Suzuki, A. and Hashimoto, M. *J. Appl. Polym. Sci.* 1981, **26**, 1951
- 3 Kunugi, T. 'New Materials and New Processes, Vol. 1' The U.S. Office of ECS of Japan, 1981, p 58
- 4 Kunugi, T. *Sen i Gakkaishi* 1980, **36**, 411
- 5 Kunugi, T. *Chem. Ind. (Japan)* 1981, **32**, 289
- 6 Kunugi, T., Suzuki, A., Akiyama, I. and Hashimoto, M. *Polym. Prepr. Am. Chem. Soc.* 1979, **20**, 778
- 7 Kunugi, T., Akiyama, I. and Hashimoto, M. *Polymer* 1982, **23**, 1193
- 8 Kunugi, T., Akiyama, I. and Hashimoto, M. *Sen i Gakkai Prepr.* p 11 (at Nagoya, Oct. 1979)
- 9 Kunugi, T., Aoki, I. and Hashimoto, M. *Kobunshi Ronbunshu* 1981, **38**, 301
- 10 Kunugi, T., Aoki, I., Hashimoto, M. and Kakiuchi, S. *The 11th Chukaren. Prepr.* p 353 (at Nagoya, Oct. 1980)
- 11 Kunugi, T., Ootaki, N., Ito, T., Ooishi, S. and Hashimoto, M. *Sen i Gakkai Prepr.* p 54 (at Tokyo, May 1981)
- 12 Holmes, D. R., Bunn, C. W. and Smith, D. J. *J. Polym. Sci.* 1955, **17**, 159
- 13 Roldan, L. G. and Kaufman, G. S. *J. Polym. Sci.* 1963, **B-1**, 603
- 14 Hashimoto, M., Kunugi, T., Otagiri, N. and Amemiya, K. *Nippon Kagaku Kaishi* (J. Chem. Soc. Japan) 1972, 454
- 15 Kunugi, T., Yokokura, S. and Hashimoto, M. *Nippon Kagaku Kaishi* 1976, 278
- 16 Sakurada, I. and Kaji, K. *J. Polym. Sci. C* 1970, **31**, 57
- 17 Kunugi, T., Iwasaki, H. and Hashimoto, M. *Nippon Kagaku Kaishi* 1981, 149
- 18 Peterlin, A. *J. Polym. Sci. A-2* 1969, **7**, 1151